



Performance and First Physics Results of the SVT Trigger at CDF II

I. Vila
for the CDF Collaboration.

IFCA (Universidad de Cantabria - Consejo Superior de Investigaciones Científicas), 39005 Santander - Spain

For the first time in a hadron collider, a novel trigger processor, the Silicon Vertex Trigger (SVT), allows to select the long-lived heavy flavor particles by cutting on the track impact parameter with a precision similar to that of the offline reconstruction. Triggering on displaced tracks has enriched the B-physics program by enhancing the B yields of the lepton-based triggers and opened up full hadronic triggering at CDF. After a first commissioning period, the SVT is fully operational, performing very closely to its design capabilities. System performance and first physics results based on SVT selected data samples are presented.

1 Introduction

The upgraded Collider Detector at Fermilab (CDF) at the $p\bar{p}$ Tevatron collider is back in operation since March 2001. A detailed description of the upgraded detector can be found elsewhere [1]. New vertexing, triggering and particle identification capabilities have been added enhancing the potentialities of the B physics program [2].

There are several motivations for pursuing B physics at a $p\bar{p}$ collider at $\sqrt{s} = 1.96 \text{ TeV}$. The first reason is the three orders of magnitude higher production rate of B hadrons with respect to the conventional B experiments in e^+e^- colliders at the $\Upsilon(4S)$ or at the Z^0 pole. This huge B production cross section allows searches for the very rare B decays and performing precise B physics measurements. Another important advantage is the fact that all the B hadron species are produced, in contrast with the e^+e^- machines at the $\Upsilon(4S)$ experiments where only the B^+ and B_d^0 are created.

However, QCD backgrounds in a hadronic experiment are also three orders of magnitude higher, therefore dedicated triggers for suppressing the background are needed. For the first time in a hadron detector, a novel Silicon Vertex Trigger (SVT) is being used. This new level-2 trigger processor allows to select the long-lived heavy flavor particles by cutting on the track impact parameter with a precision similar to that achieved by the full event offline reconstruction.

In the following sections, a brief description of the SVT, its performance and first physics results are given.

2 SVT Overview

2.1 CDF trigger system and SVT functionalities

The CDF trigger system has also been upgraded to accommodate the new bunch spacing (396 ns) and larger luminosity ($\sim 10^{32} \text{ cm}^2\text{s}^{-1}$). The CDF Trigger is a three level

pipelined and buffered system. The first level is a dead-timeless pipelined synchronous system with a present accept rate of about 20 kHz and a pipeline depth of $5.5 \mu\text{s}$. The first level trigger decision is made using the transverse energy of the calorimeter, tracks in the central drift chamber and track segments in the muon system. The second level trigger is an asynchronous system with a latency of $\sim 30 \mu\text{s}$ and a current accept rate of 300 Hz. It is structured as a two stage pipeline with data buffering at the input of each stage. The first stage is based on dedicated hardware processors which assemble information from a particular section of the detector (Calorimeter Clusters, Silicon tracks, etc). The second stage consists of programmable processors (DEC Alpha processors) operating on lists of objects generated by the first stage. Each of the L2 stages is expected to take approximately half of the total level-2 latency. The SVT works inside the first stage of this trigger level. The final selection is done by the level-3 event filter, a farm of about 250 Linux PCs which performs the full event reconstruction, reducing typically to $\sim 50 \text{ Hz}$ the writing rate to permanent storage.

The SVT is a data driven trigger processor at the level-2 of the CDF trigger system, dedicated to the 2-D reconstruction of charged particle trajectories in a plane perpendicular to the beam line [3]. The SVT inputs are the sparsified list of channel numbers from four layers of the Silicon Vertex detector (SVX II) [4] with its corresponding pulse amplitudes, and the tracks reconstructed in the central drift chamber (COT) [5] by the new level-1 trigger processor, the eXtremely Fast Tracker (XFT) [6]. With a latency of only $1.9 \mu\text{s}$, the XFT finds and fits COT tracks of transversal momentum larger than 1.5 GeV with a tracking efficiency of 96%. The SVT output is a list of reconstructed tracks with a core resolution of the track parameters very similar to that of the offline track reconstruction.

The SVT performs SVX II hit finding, pattern recognition and track fitting in about $15 \mu\text{s}$ within the time window of the level-2 first stage latency. The key design features to accomplish these tasks in such a short time interval

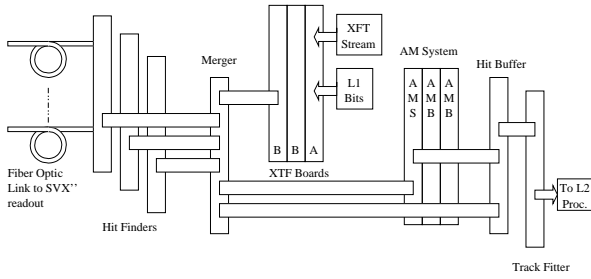


Figure 1. Board organization of an SVT sector (1/12 of the whole system) .

are a *highly parallel design* (architecture and tasking), a *pipelined architecture*, a *custom VLSI pattern recognition* and *linearized fitting* of the particle candidate trajectories.

2.2 System architecture and data processing

The SVT has been implemented on custom design VME 9U boards, organized in 12 identical subsystems (sectors) running independently in parallel. This segmentation maps the SVX II geometry, which is divided into 12 identical wedges along the azimuthal angle. The main functional blocks of each SVT sector are the Hit Finders, the Associative Memory system, the Hit Buffer and the Track Fitter, see Fig. 1.

Raw SVX II data flow from the front-end to the Hit Finder boards that find clusters of strips with a significant energy deposit and compute the coordinate of the centroids (hits). The curvature and the azimuthal angle of COT tracks from the XFT are received, fanned out to the 12 SVT sectors and fed both to the Associative Memory and to the Hit Buffer boards together with the SVX II hits. The Associative Memory boards find coincidences between the SVX II hits and a set of predefined patterns of particle trajectories. To reduce the amount of required memory to store those trajectory templates, the pattern recognition process is performed at a coarser resolution than the full available detector resolution, choosing a SuperStrip size of $250 \mu\text{m}$ for the silicon layers and 5° for the azimuthal XFT track angle.

The output of the Associative Memory system is the list of track candidates (roads), which are sent to the Hit Buffer. Each Hit Buffer stores all hits and tracks in a sector for each event, then retrieves the hits and the XFT tracks belonging to each road and sends them to the Track Fitter boards that perform quality cuts and estimate track parameters using the full available spatial resolution in a linearized fit.

A set of Merger boards, each providing 4-way fan-in and 2 way fan-out, ties together all boards in a chain that starts from 144 optical links from the SVX II, 1 Gbit/s each, and ends in a single data path, a 0.7 Mbit/s LVDS cable, to the CDF level-2 processor.

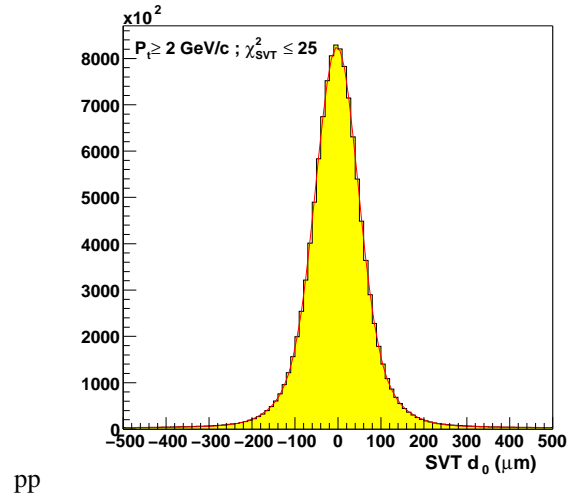


Figure 2. SVT tracks impact parameter distribution.

2.3 SVT Performance

The SVT performance has been evaluated with data samples selected by triggers which do not require SVT information, like the "dimuon" or "minimum bias" trigger paths, to avoid any possible bias on the results.

The precise determination of the transverse impact parameter of the SVT tracks requires the previous knowledge of the actual beam line position, the real SVX II geometry and the relative position between the central drift tracker chamber and the SVX II. Originally, the baseline plan was to steer the Tevatron beam to its nominal position using the SVT as a beam position monitoring device. It turns out to be more convenient to do a real-time determination of the beam position (computed every 30 s), using the SVT built-in data monitoring and diagnosis capabilities, and correct the fitted track parameters in an event by event basis, avoiding the need of modifying the beam orbit.

The impact parameter distribution of the SVT tracks corrected by SVX II alignment and the beam line position is shown in Fig. 2. The distribution width $\sim 50 \mu\text{m}$ results from the convolution of $35 \mu\text{m}$ SVT resolution and the beam spot with a $33 \mu\text{m}$ width.

The overall SVT tracking efficiency is about 80%. This efficiency is defined as the ratio between the number of SVT tracks and the number of offline tracks matched to a XFT track in the SVT fiducial volume. No tracking efficiency dependence on the transverse momentum of the tracks is observed.

In the case of the efficiency dependence on the impact parameter of the tracks, shown in Fig. 3, we observe a sharp drop in the efficiency for impact parameter values beyond 0.1 cm. This effect is due to the finite number of predefined road patterns that can be stored in the Associative Memory boards. A new improved pattern set, which accounts for a larger than expected shift between the SVX II and the COT,

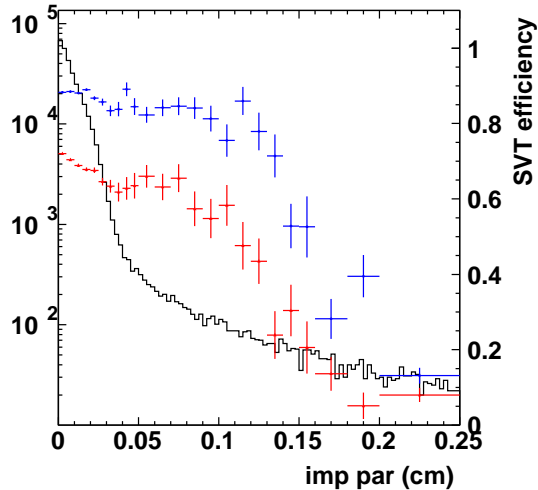


Figure 3. SVT tracking efficiency dependence on track impact parameter. The distribution of tracks is shown in black, the SVT efficiency with the initial (new) road patterns in clearer (darker).

and the beam line offset, has increased by $\sim 10\%$ the initial SVT overall tracking efficiency. The other significant efficiency improvement comes from the SVX II acceptance recovery.

There is always the possibility that random combinations of SVX II hits which do not correspond to real tracks pass the SVT track quality cuts producing fake tracks. The overall SVT track purity is about 80%; the purity is close to 100% for primary tracks and gets lower for high impact parameter tracks.

3 Initial Physics Signals

Conventionally, triggering on dimuons coming from J/ψ or semileptonic b decays was the only way to do heavy flavor physics at hadron colliders. The SVT has opened the new way of fully hadronic decay triggering, and expanded the semileptonic trigger. The initial experience with the SVT has been very successful, allowing for competitive results even with a modest amount of integrated luminosity.

3.1 Semileptonic trigger

The enhanced semileptonic trigger selects events with a lepton of transverse momentum $p_T > 4 \text{ GeV}$, and a displaced track with an impact parameter $100 \mu\text{m} < d_0 < 1 \text{ mm}$ with $p_T > 2 \text{ GeV}$. The additional displaced track requirement allows for a lower lepton p_T cut, increasing the collected sample size. For a total integrated luminosity of about 70 pb^{-1} there are more than half a million recorded inclusive semileptonic decays, a yield five times larger than the Run I equivalent semileptonic trigger. For the same

luminosity, the number of partially reconstructed semileptonic charmed b decays, like $B \rightarrow ID^0 X$ ($D^0 \rightarrow K\pi$), $B \rightarrow ID^* X$ ($D^* \rightarrow D^0\pi$) and $B \rightarrow ID^+ X$ ($D^+ \rightarrow K\pi\pi$) is about 10000, 1500 and 5000 events respectively. These samples are used for flavor tagging optimization and measurements of B_d mixing and life times.

3.2 Fully hadronic trigger

The hadronic trigger selects events with at least two displaced tracks of opposite charge with transverse momentum $p_T > 2 \text{ GeV}$ and $\sum p_T > 5.5 \text{ GeV}$. It comes in two flavors for two different event topologies: the two-body decay trigger with an impact parameter cut of $100 \mu\text{m} < d_0 < 1 \text{ mm}$ and large opening angle between trigger tracks, and the multibody decay trigger with tighter impact parameter cut ($120 \mu\text{m} < d_0 < 1 \text{ mm}$) and smaller opening angle. Tracks originating from tertiary decay vertexes in a multibody decay will have on average larger impact parameters than tracks from the secondary decay vertexes in a two-body decay.

Originally, the hadronic trigger was designed for collecting fully hadronic b decays. It turns out to be also very efficient collecting charm hadronic decays.

In the following sections, we will give a brief summary of the main initial charm and b physics results based on the SVT hadronic trigger.

3.2.1 Charm physics results

The measurement of the prompt D meson cross section is of theoretical interest to clarify the larger than expected beauty cross section compared to the next-to-leading order QCD calculations. A preliminary measurement of the D meson cross sections was done with a total integrated luminosity of 5.7 pb^{-1} . The production cross sections were found to be larger than the corresponding bottom meson cross sections: $4.3 \pm 0.1 \pm 0.7 \mu\text{b}$ for D^+ and $9.3 \pm 0.1 \pm 1.1 \mu\text{b}$ for D^0 .

The measurement of the $m_{D_s^+} - m_{D^+}$ mass difference provides a test for the Heavy Quark Effective Theory and QCD. The analysis required the precise calibration of the momentum scale of the detector using a sample of 50000 $J/\Psi \rightarrow \mu\mu$ decays. The calibration was applied to the decays $D_s^+, D^+ \rightarrow \phi\pi^+$ and the mass difference value found was $m_{D_s^+} - m_{D^+} = 99.41 \pm 0.38(\text{stat.}) \pm 0.21(\text{syst.}) \text{ MeV}/c^2$ [7]. Figure 4 shows the invariant mass distribution of the two signals.

Observation of large CP violation in the charm system would be an evidence of new physics beyond the Standard Model. In a sample of $65 \pm 4 \text{ pb}^{-1}$, the Cabibbo-suppressed decays to CP eigenstates $D^0 \rightarrow K^+K^-$ and $D^0 \rightarrow \pi^+\pi^-$ were reconstructed. All the D^0 were selected originating from a D^{*+} decay $D^{*+} \rightarrow D^0\pi^+$ which

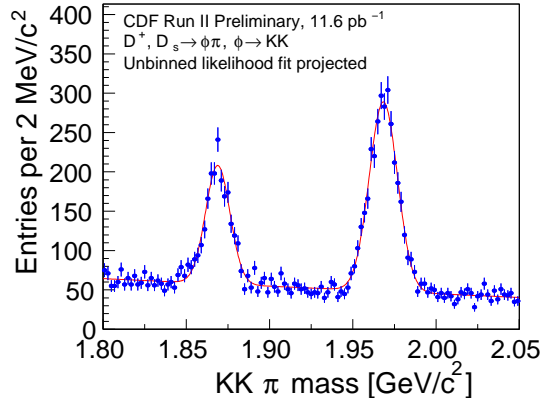


Figure 4. Invariant mass distribution for D_s^+ , $D^+ \rightarrow \phi\pi$ signals with superimposed fit.

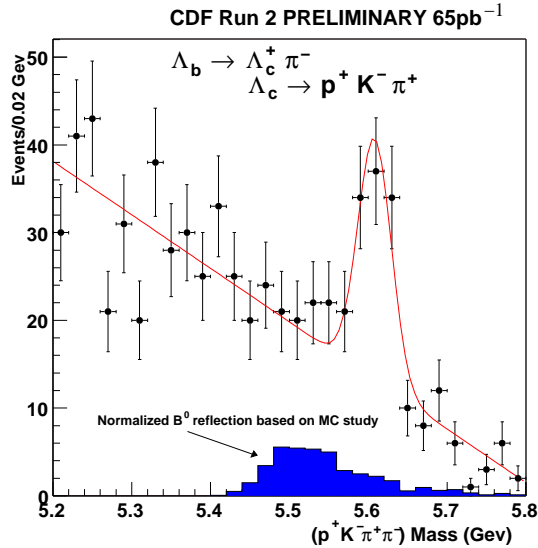


Figure 5. Λ_b signal reconstructed in the $\Lambda_b \rightarrow \Lambda_c^+ \pi^-$ channel.

provides a very pure and flavor tagged sample. The direct CP asymmetries $A = \frac{\Gamma(\bar{D} \rightarrow \bar{f}) - \Gamma(D \rightarrow f)}{\Gamma(\bar{D} \rightarrow \bar{f}) + \Gamma(D \rightarrow f)}$ were found to be $2.0 \pm 1.7(stat.) \pm 0.6(syst.)\%$ for $D^0 \rightarrow K^+ K^-$ and $3.0 \pm 1.9(stat.) \pm 0.6(syst.)\%$ for $D^0 \rightarrow \pi^+ \pi^-$ decay modes.

3.2.2 Beauty physics

Initially purely hadronic b decays have been established, and currently we are in the process of understanding the signal yields. In particular, events for the B_s mixing golden channel $B_s \rightarrow D_s \pi$ has been observed [8]. Fully reconstructed Λ_b 's has been collected, using the $\Lambda_b \rightarrow \Lambda_c^+ \pi^-$ decay with $\Lambda_c \rightarrow p^+ K^- \pi^+$. In Fig. 5. the Λ_b invariant mass distribution is shown.

The charmless purely hadronic two-body decay of neutral B mesons has been reconstructed. The invariant mass distribution of two tracks of opposite charge, assuming the

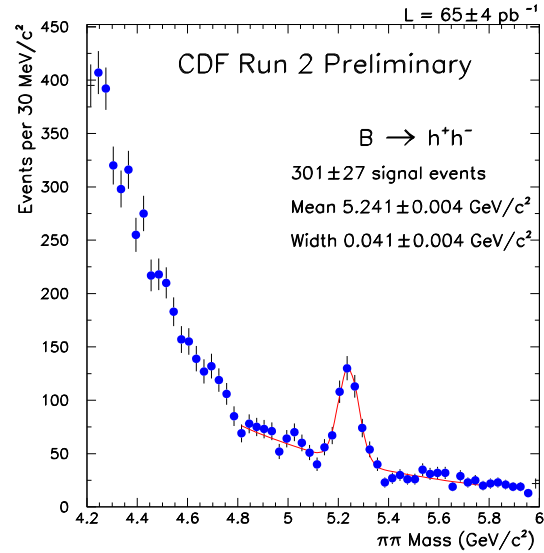


Figure 6. Invariant mass distribution for $B \rightarrow h^+ h^-$ signals with superimposed fit

pion hypothesis for each track, is shown in Fig.6. The mass peak is a mixture of $B^0, B_s \rightarrow \pi\pi, K\pi, KK$ decays. The contribution of each decay mode has been disentangled with discriminating cuts based on track dE/dx and kinematics. The physics interests of this measurement are, among others, the first evidence of charmless B_s decays, direct CP asymmetry measurements in $B^0 \rightarrow K^+ \pi^-$ and CP asymmetry in $B^0 \rightarrow \pi\pi$.

References

1. The CDF-II Collaboration, FERMILAB-PUB-96-390-E, Nov 1996.
2. R.G.C Oldeman, *Performance of CDF for B physics*, these proceedings.
3. W. Ashmanskas et al., IEEE Trans.Nucl.Sci. 49, 1177 (2002).
4. A. Sill [CDF Collaboration], Nucl. Instrum. and Meth. A 447, 1 (2000).
5. K.T. Pitts[CDF Collaboration], Nucl. Phys. Proc. Suppl. 61B, 230 (1998).
6. E. J. Thomson et al., IEEE Trans. Nucl. Sci. 49, 1063 (2002).
7. D. Acosta et al.[CDF-II Collaboration], Measurement of the Mass Difference $m(D_s^+) - m(D^+)$ at CDF II. Submitted to Phys. Rev. D.
8. D Lucchesi, B_s Physics and Prospects at the Tevatron, these proceedings.